HHS Public Access

Author manuscript

Ultrasound Med Biol. Author manuscript; available in PMC 2019 February 01.

Published in final edited form as:

Ultrasound Med Biol. 2018 February ; 44(2): 321–331. doi:10.1016/j.ultrasmedbio.2017.10.010.

An ultrasound surface wave technique for assessing skin and lung diseases

Xiaoming Zhang, PhD[1,2], **Boran Zhou, PhD**[1], **Sanjay Kalra, MD**[3], **Brian Bartholmai, MD**[1], **James Greenleaf, PhD**[2], and **Thomas Osborn, MD**[4]

[1]Department of Radiology, Mayo Clinic, Rochester, MN 55905, USA

[2]Department of Physiology and Biomedical Engineering, Mayo Clinic, Rochester, MN 55905, USA

[3]Department of Pulmonary and Critical Care Medicine, Mayo Clinic, Rochester, MN 55905, USA

[4]Department of Rheumatology, Mayo Clinic, Rochester, MN 55905, USA

Abstract

Systemic sclerosis (SSc) is a multi-organ connective tissue disease characterized by immune dysregulation and organ fibrosis. Severe organ involvement, especially of the skin and lung, is the cause of morbidity and mortality in SSc. Interstitial lung disease (ILD) includes multiple lung disorders in which the lung tissue is fibrotic and stiffened. The purpose of this study was to translate ultrasound surface wave elastography (USWE) for assessing patients with SSc and/or ILD via measuring surface wave speeds of both skin and superficial lung tissue. 41 patients with both SSc and ILD and 30 healthy subjects were enrolled in this study. An external harmonic vibration was used to generate the wave propagation on the skin or lung. Three excitation frequencies of 100 Hz, 150 Hz, and 200 Hz were used. An ultrasound probe was used to measure the wave propagation in the tissue noninvasively. Surface wave speeds were measured on the forearm and upper arm of both left and right arms as, well as, the upper and lower lungs through six intercostal spaces of patients and healthy subjects. Viscoelasticity of the skin was calculated by the wave speed dispersion with frequency using the Voigt model. The magnitudes of surface wave speed and viscoelasticity of patients' skin were significantly higher than those of healthy subjects ($p<0.0001$) for each location and each frequency. The surface wave speeds of patients' lung were significantly higher than those of healthy subjects ($p<0.0001$) for each location and each frequency. USWE provides a noninvasive and nonionizing technique to measure both skin and lung surface wave speed, which may be useful for quantitative assessment of SSc and/or ILD.

Keywords

ultrasound surface wave elastography (USWE); skin; lung; scleroderma; interstitial lung disease (ILD)

Corresponding Author: Xiaoming Zhang, PhD, Associate Professor, Department of Radiology, Mayo Clinic, 200 1st ST SW, Rochester, MN 55905, USA, Phone: 507-538-1951, Fax: 507-266-0361, zhang.xiaoming@mayo.edu.

INTRODUCTION

Systemic sclerosis (SSc), also termed scleroderma, is a multi-organ connective tissue disease characterized by immune dysregulation and organ fibrosis (Steen and Medsger 2000). Thickening of the skin, often the earliest affected organ, is considered an early marker of disease activity in SSc (Steen and Medsger 2000). Severe organ involvement, especially of the skin and lung, is the cause of morbidity and mortality in SSc. The degree of skin involvement is a predictor of mortality (Clements, et al. 1990). Improvement in skin stiffness is associated with improved survival in many clinical trials (Steen and Medsger 2001). Patients who do not develop severe organ involvement in the first few years are less likely to develop life-threatening involvement later throughout the course of the disease. The Modified Rodnan Skin Score (MRSS) is the standard skin assessment tool in the majority of clinical studies of SSc (Abignano, et al. 2011). It shows that patients with improved MRSS after two years of treatment had improved survival (Steen and Medsger 2001). The MRSS is commonly used as an outcome measure in clinical trials (Clements, et al. 2000). However, the MRSS is a palpation method, which is subjective, and thus, its accuracy is user-dependent (Clements, et al. 1995). Moreover, it is difficult to measure the change of skin stiffness over time using palpation (Postlethwaite, et al. 2008).

Skin stiffness can be measured using durometry (Kissin, et al. 2006, Merkel, et al. 2008), indentation (Boyer, et al. 2009, Pailler-Mattei, et al. 2008, Serup 1995), and cutometers (Hendriks, et al. 2006, Smalls, et al. 2006). Durometry uses a piston-spring-dial handheld apparatus to measure skin hardness. However, durometry readings are affected by the experience of users. Indentation is the technique of measuring elasticity by indenting the material. The cutometer measures skin displacement in response to a suction force. Because its measurements depend on the interactions between a probe and the skin, deeper skin layers must be measured with larger probes (Hendriks, et al. 2006). Notably, these techniques cannot evaluate subcutaneous tissue.

Patients with ILD have fibrotic and stiff lungs leading to symptoms, especially dyspnea, and may eventually lead to respiratory failure (Coultas, et al. 1994). Many ILDs typically are distributed in the peripheral, subpleural regions of the lung (Desai, et al. 2004, Wells, et al. 1993). High-resolution computed tomography (HRCT) is the clinical standard for diagnosing lung fibrosis (Mathieson, et al. 1989, Verschakelen 2010), but it substantially increases radiation exposure for patients. Various scanning techniques were proposed to reduce the dose (Mayo 2009). Intercostal ultrasound can be used to avoid ionizing radiations during follow-ups (Delle Sedie, et al. 2012). However, it is not able to quantify the stiffness of lung.

Currently, no clinical approach is available to noninvasively quantify and evaluate the progression and development of SSc and ILD. Therefore, there is a pressing need to develop an accurate and reproducible clinical technique of quantification, tracking of the disease, and developing effective treatment for sclerosis and fibrotic disorders. (Lott and Girardi 2011). This research aims to translate an ultrasound surface wave elastography (USWE) technique

into clinical use for quantitatively assessing patients with SSc and interstitial lung disease (ILD).

METHOD

Raleigh Surface Wave Equation

Surface wave propagation can be analyzed as wave propagation in a semi-infinite linear elastic medium under a local harmonic excitation on the surface. The equation for wave propagation in an isotropic and elastic medium is (Miller 1954)

$$(\lambda+2\mu)\nabla\nabla.\vec{u}-\mu\nabla\times\nabla\times\vec{u}=\rho\frac{\partial^2\vec{u}}{\partial t^2}, \quad (1)$$

where $\vec{u}$ is the displacement vector, ρ is the mass density, and λ and μ are, respectively, the Lamé coefficients of the medium. For linear viscoelastic material, $\lambda = \lambda_1 + \partial\lambda_2/\partial t$ and $\mu = \mu_1 + \partial\mu_2/\partial t$, where λ_1, λ_2, μ_1 and μ_2 are the coefficients of volume compressibility, volume viscosity, shear elasticity and shear viscosity, respectively.

The surface wave propagation can be solved in the cylindrical polar coordinate system as shown in Fig. 1. Consider a harmonic force excitation with a uniform stress on the surface of the medium in the circular region of $r \le a$. The displacement fields are derived in the r and z directions at any location in and on the surface of the medium as (Miller 1954),

$$u_z=\frac{a}{\mu}\int_0^\infty\frac{\sqrt{(\xi^2-1)}J_1(\xi k_1 a)}{F_0(\xi)}\{2\xi^2 e^{-k_1 z\sqrt{(\xi^2-\eta^2)}}+(\eta^2-2\xi^2)e^{-k_1 z\sqrt{(\xi^2-1)}}\}J_0(\xi k_1 r)d\xi$$

$$u_r=\frac{a}{\mu}\int_0^\infty\frac{\xi J_1(\xi k_1 a)}{F_0(\xi)}\{2\sqrt{(\xi^2-1)}\sqrt{(\xi^2-\eta^2)}e^{-k_1 z\sqrt{(\xi^2-\eta^2)}}+(\eta^2-2\xi^2)e^{-k_1 z\sqrt{(\xi^2-1)}}\}J_1(\xi k_1 r)d\xi, \quad (2)$$

where a is the radius of the distributed stress, and ξ is the integration parameter in the wave number domain, which has been normalized with respect to k_1. The divisor function of the integration functions is $F_0(\xi)=(2\xi^2-\eta^2)^2-4\xi^2\sqrt{(\xi^2-1)}\sqrt{(\xi^2-\eta^2)}$, where $\eta=k_2/k_1=\sqrt{\{2(1-\sigma)/(1-2\sigma)\}}$, $k_1=\omega\sqrt{\rho/(\lambda+2\mu)}$, $k_2=\omega\sqrt{\rho/\mu}$, where ω is the angular frequency, ρ is the density, σ is the Poisson's ratio for the medium, k_1 and k_2 denote the wave numbers for compression and shear wave propagation, respectively, J_0 and J_1 refer to Bessel functions of the first kind.

The wave displacement fields can be solved with equation (2). However, using the displacements to estimate the elastic properties of the medium depends on the excitation and

boundary conditions. Since the wave propagation is dependent on local medium properties, we used the surface wave speed measurement to estimate the viscoelastic properties of the medium. The surface wave speed can be solved by (Zhang and Greenleaf 2007)

$$(2\xi^2-\eta^2)^2-4\xi^2\sqrt{(\xi^2-1)}\sqrt{(\xi^2-\eta^2)}=0. \quad (3)$$

Equation (3) is a bi-fourth equation of ξ, however, only the solution for which ξ is real, $\xi > \eta$ and $\xi > 1$ is the right solution for the surface wave.

Equation (3) has been studied by (Nkemzi 1997) and us (Zhang and Greenleaf 2007). Several approximations have been proposed to solve the surface wave speed (Royer and Clorennec 2007, Twal, et al. 2014, Viktorov 1976, Vinh and Malischewsky 2007). The following equation approximates the relationship between the shear wave speed c_2 and the surface wave speed c_s (Royer and Clorennec 2007),

$$\frac{c_2}{c_s}=\sqrt{\frac{0.58+K}{0.44+K}}, \quad (4)$$

where $K = \sigma / (1 - \sigma)$, σ is the Poisson's ratio of the medium. The speed of shear wave is slightly greater than that of surface wave for all materials from metals to soft tissues. Because soft tissues are generally incompressible and their Poisson's ratios are in a narrow region between 0.45 and 0.50, $c_2 = 1.05\ c_s$ can be obtained from equation (4). The surface wave speed can be related to the elastic modulus of tissue as (Zhang and Greenleaf 2007),

$$c_s=\frac{1}{1.05}\sqrt{\frac{\mu}{\rho}} \quad (5)$$

where μ is the shear elasticity in Pascal and ρ is the mass density of the tissue in kg/m^3.

Voigt's Viscoelastic Model – Wave Dispersion Curve

For soft tissue under low frequency harmonic excitation, the Voigt's model, which consists of a spring of elasticity μ_1 and a damper of viscosity μ_2 connected in parallel, has been proven to be effective in modeling the linear viscoelastic materials (Catheline, et al. 2004, Chen, et al. 2009, Prim, et al. 2016, Zhou, et al. 2017). The wave dispersion curve of wave speed c_s with respect to the excitation frequency ω can be formulated by,

$$c_s=\frac{1}{1.05}\sqrt{\frac{2(\mu_1^2+\omega^2\mu_2^2)}{\rho(\mu_1+\sqrt{\mu_1^2+\omega^2\mu_2^2})}}. \quad (6)$$

Cross-spectrum - Phase Gradient Method

In USWE, a 0.1s harmonic vibration at a frequency is generated on the skin and the resulting time response of the skin is measured using an ultrasound probe. Let $s_1(t)$ and $s_2(t)$ represent the displacement responses at two locations on the skin, the phase change of surface wave propagation over the two locations can be calculated with a cross-spectrum method. The cross-spectrum $S(f)$ of two signals $s_1(t)$ and $s_2(t)$ is defined as (Hasegawa and Kanai 2006),

$$S(f)=S_1^*(f)\cdot S_2(f)=|S_1(f)\cdot S_2(f)|\cdot e^{-j\Delta\varphi(f)}, \quad (7)$$

where $S_1(f)$ and $S_2(f)$ are the Fourier transforms of $s_1(t)$ and $s_2(t)$, respectively; * denotes the complex conjugate and $\Delta\phi(f)$ is the phase change between $s_1(t)$ and $s_2(t)$ over distance at frequency f.

The phase change of surface wave with distance is used to measure the surface wave speed,

$$c_s=2\pi f|\Delta r/\Delta\phi|, \quad (8)$$

where Δr is the radial distance of two measuring locations, $\Delta\phi$ is the wave phase change over distance, and f is the frequency.

The estimation of wave speed can be improved by using multiple phase change measurements over distance. The regression of the phase change $\Delta\phi$ with distance Δr can be obtained by "best fitting" a linear relationship between them, and the equation is

$$\Delta\phi=\alpha\Delta r+\beta, \quad (9)$$

where $\Delta\phi$ denotes the value of $\Delta\phi$ on the regression for a given distance of Δr, and α is the regression parameter.

The surface wave speed can be estimated by

$$c_{\mathrm{sr}}=2\pi f\,|\Delta r/\Delta\phi|=2\pi f/\alpha, \quad (10)$$

where c_{sr} is the estimation of wave speed from the regression analysis.

Human Study Protocol

Human studies were approved by the Mayo Clinic Institutional Review Board (IRB). Each participant completed an informed consent form. Patients were enrolled in this research based on their clinical diagnoses. 41 patients with SSc and ILD were enrolled from Mayo Clinic Departments of Rheumatology and Pulmonary and Critical Care Medicine. These patients are confirmed ILD patients with clinical assessments together with pulmonary function test and high resolution CT scans. These patients also have confirmed clinic diagnosis of SSc. The American College of Rheumatology (ACR) (1980) developed

classification criteria for SSc in 1980. The diagnosis requires either 1) the major criterion of proximal scleroderma, as judged by palpating or simply observing the skin; or 2) 2 minor criteria such as sclerodactyly, digital pitting scars, or loss of substance from the finger pad, and bibasilar pulmonary fibrosis. The patients enrolled in this study typically have advanced disease because fibrosis already involves the two organs of skin and lung. Further analysis of disease severity and grading using the surface wave speed measures is being carried out and will be published soon. Patients' mean age was 61.88 years (range 37–82, 13 male and 28 female). 30 healthy subjects were enrolled as controls if they did not have any skin or lung diseases. Controls' mean age was 45.43 years (range 22–73, 14 male and 16 female).

A subject was tested in a sitting position while his/her left or right forearm and upper arm were placed horizontally on a pillow in a relaxed state. The skin of both left and right forearms and upper arms of subjects was tested (Fig. 2). These locations were in the central part of the arms and on the dorsal sides. A 0.1-second harmonic vibration was generated by the indenter of the handheld shaker (Model: FG-142, Labworks Inc., Costa Mesa, CA 92626, USA) on the skin of the forearm or upper arm of the subject. The excitation force from the indenter was much less than 1 Newton and the subject only felt a small vibration on his/her skin. A Verasonics ultrasound system (Verasonics V1, Verasonics, Inc., Kirkland, WA 98034, USA) with an ultrasound probe of L11-4 with a central frequency of 6.4 MHz was used for detecting the surface wave motion of the skin. The probe had an elevation aperture of 38.4 mm and was customized to provide a 50-mm focal depth in the elevation axis. Elements were spaced at 30 μm intervals along the azimuthal axis. All images were acquired at a 50 V transmission voltage. Images of the skin and lung tissue were acquired by compounding 11 successive angles at a pulse repetition frequency (PRF) of 2 kHz. In order to improve the imaging quality of skin, an ultrasound gel pad standoff by Aquaflex® (Parker Laboratories, Inc., Fairfield, NJ 07004, USA) was placed between probe and skin. Surface wave speed on the skin was measured by determining the change in wave phase with distance along the skin. Figure 3 shows representative B-mode images of the skin for a patient and a healthy subject. The top dark area of the image shows the Aquaflex® standoff gel pad. On the skin surface, eight locations were used to measure the surface wave speed of skin. The skin motion velocity was in response to the external vibration excitation induced by the handheld vibrator. Using the skin motion at the first location as a reference, the wave phase delay of the skin motions at the remaining locations, relative to the first location, was used to measure the surface wave speed. The surface wave speed was measured at three excitation frequencies of 100 Hz, 150 Hz, and 200 Hz. Three measurements were performed at each location and at each frequency. A small tissue motion in tens of μm was enough for sensitive ultrasound detection of the generated tissue motion. The 100 Hz excitation signal is stronger than those of higher frequency excitations. The higher frequency waves have smaller wave length but decay more rapidly over distance than the lower frequency waves. The frequency ranges chosen in this study consider the wave motion amplitude, spatial resolution, and wave attenuation.

We studied repeatability and reproducibility of the USWE measurements on the forearm of a healthy subject. Ten measurements of wave speed were performed at 100 Hz, 150 Hz, and 200 Hz. The inter-rater reliability was evaluated by two rater's measurements. The inter-class correlations (ICCs) were 0.94, 0.96, and 0.98 for wave speeds at 100 Hz, 150 Hz, and

200 Hz, respectively. The intra-rater reliability was evaluated by the same rater's measurements at one day and one week later. At that time, the ICCs were 0.95, 0.91, and 0.95 for wave speeds at 100 Hz, 150 Hz, and 200 Hz, respectively. In these measurements, there were no statistical differences of the mean measurements between the intra-rater and inter-rater data. Reproducibility and repeatability is considered "good" for ICCs ≥0.60 and ≤0.74, and "excellent" for ICCs ≥0.75 and ≤1.00 (Cicchetti 1994).

Both lungs of the subject were tested through six intercostal spaces. The upper anterior lungs were tested at the second intercostal space in the mid-clavicular line. The lower lateral lungs were tested at one intercostal space above the level of the diaphragm in the mid-axillary line. The lower posterior lungs were tested at one intercostal space above the level of the diaphragm in the mid-scapular line. The indenter of the handheld shaker is placed on the chest wall in an intercostal space. The same ultrasound system and probe were used for lung testing. The ultrasound probe is positioned about 5 mm away from the indenter in the same intercostal space to measure the resulting surface wave propagation on the lung. The lung was tested at total lung capacity in which the subject took a deep breath and held for a few seconds. Ultrasound imaging was used to identify the lungs and select appropriate intercostal spaces to measure the upper and lower lungs. Three measurements were performed at each location and at each frequency. Typical testing lasted about 30 minutes.

In lung testing, a direct vibration excitation on the lung surface is not possible. Instead, the surface wave propagation on the lung is induced by a vibration excitation on the chest wall. The resulting wave propagates through the intercostal muscle and on the surface of the lung. We previously demonstrated that surface wave propagation on the lung can be generated by a vibration excitation on the surface of muscle in an *ex vivo* muscle-lung model (Zhang, et al. 2016).

Statistical analysis

An unpaired, two-tailed *t*-test between the healthy subjects and patients was conducted to compare the sample means. Differences in mean values were considered significant when $p<0.05$.

RESULTS

Figure 4 shows a representative wave speed at 100 Hz for a healthy subject and a patient at the same location. The representative surface wave speeds were, respectively, 3.69 m/s and 1.97 m/s for the patient and the healthy subject. Three measurements were made for each frequency and at each location. Table 1 shows representative measurements of surface wave speed for a healthy subject and a patient. The surface wave speed is shown in the format of mean ± SD for the three measurements at each location and each frequency. The forearm and upper arm are designated by numbers 4 and 5, respectively. The right and left arms are designated by letters R and L, respectively. Therefore, R4 represents the skin of the right forearm.

A comparison of wave speeds between 30 healthy subjects and 41 patients is shown in Figure 5 for 100 Hz, 150 Hz, and 200 Hz. The p-values for the *t*-test were less than 0.0001 for all four locations and three frequencies between the patients and controls, respectively.

Figure 6 shows the comparison of elasticity and viscosity of skin tissue between the 30 healthy subjects and 41 patients. Viscoelasticity is estimated using equation (6) with wave speed measurements at 100 Hz, 150 Hz, and 200 Hz. Most soft tissues have a mass density close to 1.0 g/cm^3. In this paper, the mass density of skin is assumed to be 1.0 g/cm^3. The p-values for the *t*-test were less than 0.0001 for the four locations between the patients and controls. Therefore, the magnitudes of both elasticity and viscosity of patients were statistically higher than those of healthy subjects.

Figure 7 shows representative ultrasound images of superficial lung tissue for a patient and a healthy subject. The lung surface of a healthy subject is typically smooth while a patient's lung surface is relatively rough. Table 2 shows representative measurements of surface wave speed of lung for a healthy subject and a patient. The three intercostal spaces are designated by a number from 1 to 3. The upper anterior lung is designated by 1. The lower lungs at the lateral and posterior positions are designated by 2 and 3, respectively. The right and left side of the lung are designated by letters R and L, respectively. Therefore, L1 represents the left anterior lung in the second intercostal space.

A comparison of wave speeds of lung surface between 30 healthy subjects and 41 patients is shown in Figure 8 for 100 Hz, 150 Hz, and 200 Hz. The p-values for the *t*-test were less than 0.0001 for all intercostal spaces and for three frequencies between the patients and controls, respectively.

DISCUSSION

The aim of this study was to translate an ultrasound surface wave elastography (USWE) technique into clinical use for quantitatively assessing patients with SSc and ILD. A high pulse repetition rate of 2000 frame/s was used to detect tissue motion in response to the excitations of 100, 150, and 200 Hz. A Verasonics ultrasound system was used to collect up to a few thousand imaging frames per second by using a plane-wave pulse transmission method. The skin motion velocities at these locations were measured in the normal direction of skin using the ultrasound tracking beams through those locations (Hasegawa and Kanai 2006, Zhang 2011). The wave speed on the skin was measured by analyzing ultrasound data directly from the skin. Therefore, the wave speed measurement was local and independent of the location and amplitude of excitation. The surface wave speeds of skin of both left and right forearms and upper arms of both healthy controls and SSc patients were tested at three excitation frequencies and their viscoelasticity were evaluated. The surface wave speeds of lung at six intercostal locations were measured at three excitation frequencies between healthy controls and SSc patients.

The results obtained in this study are in agreement with the published results in literature. We found the viscoelasticity of SSc patients is statistically higher than that of healthy controls. Skin of the peri-oral region of SSc patients was stiffer than that of healthy controls

(Cannaò, et al. 2014). Our earlier pilot work using an optical-based technique indicated that skin viscoelasticity was a more sensitive measure than palpation for assessing SSc (Zhang 2011). Our technology was favorably reviewed by Yale dermatologists (Lott and Girardi 2011), who commented that this novel technology could benefit patients through new multimodal paradigms for assessing SSc. Ultrasound elastography has been used to assess skin elasticity between SSc patients and healthy controls (Iagnocco, et al. 2010). However, it only provides semi-quantitative scales to characterize the elasticity of skin and it is difficult to differentiate patients from healthy subjects. USWE quantifies the viscoelasticity of skin tissue for SSc patients and provides accurate biomarkers for evaluating disease progression.

Optical coherence tomography (OCT) (Abignano, et al. 2013, Shazly, et al. 2015) and OCT-based elastography techniques (Li, et al. 2014, Nguyen, et al. 2014) provide high-spatial resolution of skin but cannot measure deep subcutaneous tissue. The imaging penetration of OCT in skin can be up to 1.5 mm (Liang and Boppart 2010). Fibrosis not only affects skin but also subcutaneous tissue (Li, et al. 2007). One advantage of USWE is its capability to measure subcutaneous tissue (Kubo, et al. 2017). In the current setup, subcutaneous tissues can be measured up to 45 mm (Figure 2, 6). USWE may be used to assess skin, subcutaneous connective tissue, and muscle for patients with SSc.

Most ultrasound-based elastography techniques use ultrasound radiation force (URF) to generate tissue motion. Acoustic radiation force impulse imaging (ARFI) has been recently used to assess skin fibrosis (Hou, et al. 2015, Lee, et al. 2015). To generate sufficient tissue motion using URF, relatively high-intensity ultrasound energy is needed. Although URF has been used in most organs including the liver, URF should not be applied to the lung. *In vivo* animal lung studies demonstrated that the relatively high-intensity ultrasound energy may cause alveolar hemorrhage or lung injury (Zachary, et al. 2006). In addition, long periods of high-intensity ultrasound may cause damage to the ultrasound system, e.g., as high voltage drop and probe element damage. In USWE, the surface wave on the lung is safely generated by a local mechanical vibration on the chest. Diagnostic ultrasound is only used for detecting surface wave propagation on the lung. Therefore, the USWE technique is a safe method for lung testing and screening patients. Moreover, because URF cannot be directly generated on surface tissue, a standoff pad is needed for exciting the skin. However, the standoff pad decays the URF and complicates the URF on the skin. In USWE, the mechanical excitation is directly applied to the skin and the standoff pad is only used to improve imaging of the skin. USWE provides a safe and simple way to generate and detect wave propagation on the skin. One advantage of USWE compared with most ultrasound elastography techniques is that the wave propagation is generated by a 0.1 second harmonic excitation rather than a short pulse using URF. The wave speed is measured quickly and accurately at a frequency with high signal-to-noise ratio. The tissue motion can be safely generated at a level of 20 μm using USWE. The radiation force ultrasound generated tissue notion is typically about 1~2 μm.

In USWE, the standoff pad is only used to improve imaging of the skin. We do not use the probe to generate the pressure on the skin such as for getting a tissue stain imaging. In our testing, the gel pad sits on the skin surface naturally. The ultrasound probe is attached to the gel pad using ultrasound gel. We keep this experimental setup for each patient. We do not

study the pressure effect on the skin measurements. However, we may investigate it by carefully controlling the generated pressure on the skin and measuring the associated surface wave speed changes. This may be useful to study nonlinear or hyperelastic properties of the skin.

The heart beat or tissue movement should not affect our skin and lung testing. The lung is tested at total lung volume when a subject takes a deep breath and holds for a few seconds. The arm's skin is tested at normal breathing and the arm is rested on a pillow. We measure the surface wave speed at a given excitation frequency between 100 Hz and 200 Hz, which is typically higher than the frequency of a heart beat or tissue movement. We use triggering for acquisition. The trigger is used to synchronize the ultrasound wave measurement with the external vibration excitation.

In this study, we measured both skin and lung surface wave speeds of patients with SSc and ILD. High-resolution computed tomography (HRCT) is the clinical standard for diagnosing and characterizing lung fibrosis (Mathieson, et al. 1989, Verschakelen 2010). However, HRCT involves ionizing x-ray radiation exposure to patients. USWE provides a noninvasive and safe method for measuring superficial lung tissues for assessing lung fibrosis (Kalra, et al. 2017, Zhang, et al. 2017). USWE may be useful as a screening tool to assess patients with ILD and compliment HRCT as a follow up tool for assessing the progression of the disease.

We cannot find the data of mass density of the lungs of ILD patients. The lung density is also dependent on the pulmonary pressure. In this research, a subject is tested at total lung capacity (TLC) when taking a deep breath and holding. In a paper using an x-ray technique (Garnett, et al. 1977), lung density was averaged to be 0.32 g/cm^3 for healthy lungs. The measurements were made with the patient sitting either on a chair or in bed and breathing quietly. Lung density was 0.33–0.93 g/cm^3 for patients with pulmonary congestion and edema. In an *ex vivo* study on sheep lungs (Jahed, et al. 1989), the lung density of 0.19–0.26 g/cm^3 was used. We expect that the lung density of ILD would be higher than that of healthy lungs. However, we were not able to find the data of lung density of ILD patients. We do not calculate lung viscoelasticity from the surface wave speeds in this paper. The surface wave speed alone provides good separation between the healthy subjects and the patients with ILD in this research. We are very interested in studying the lung density of patients with ILD and the variation of lung density with the pulmonary pressure.

USWE provides a novel, safe, noninvasive, and nonionizing technique for measuring skin and lung stiffness which may be useful for quantitative and effective assessment of both skin and lung diseases. We will further test the clinical utility of USWE in multiple fibrotic disorders. Many systemic diseases, including systemic sclerosis (SSc) (Steen and Medsger 2000), graft-vs-host disease (GVHD) (Hausermann, et al. 2008), peripheral vascular disease (Spentzouris and Labropoulos 2009), and diabetic sclerosis (Van Hattem, et al. 2008) are associated with skin stiffening due to fibrosis.

CONCLUSION

USWE provides a noninvasive and nonionizing technique to measure the surface wave speeds of both skin and superficial lung tissue. In this study, USWE was used to measure both skin and lung surface wave speeds for 41 patients with both SSc and ILD and 30 healthy subjects. The surface wave speeds were measured at four locations on the arms for three excitation frequencies of 100 Hz, 150 Hz, and 200 Hz. Viscoelasticity of the skin was calculated by the wave speed dispersion with frequency using the Voigt model. The magnitudes of surface wave speed and viscoelasticity of patients' skin were significantly higher than those of healthy subjects ($p<0.0001$). The upper and lower lungs were measured through six intercostal spaces for patients and healthy subjects. The magnitudes of surface wave speed of patient's lung were significantly higher than those of healthy subjects ($p<0.0001$) for each location and each frequency. USWE may be useful for quantitative assessment of SSc and/ or ILD. We will investigate a larger population of ILD patients to study the relationship between skin stiffness and lung stiffness for patients with and without SSc.

Acknowledgments

This study is supported by NIH R01HL125234 from the National Heart, Lung, and Blood Institute. The authors would like to thank the anonymous reviewers for their encouraging and constructive comments. We thank Mrs. Jennifer Poston for editing this manuscript. Without their assistance, this manuscript would not have been presented in the current form.

References

Preliminary criteria for the classification of systemic sclerosis (scleroderma). Subcommittee for scleroderma criteria of the American Rheumatism Association Diagnostic and Therapeutic Criteria Committee. Arthritis Rheum. 1980; 23:581–90. [PubMed: 7378088]

Abignano G, Aydin SZ, Castillo-Gallego C, Liakouli V, Woods D, Meekings A, Wakefield RJ, McGonagle DG, Emery P, Del Galdo F. Virtual skin biopsy by optical coherence tomography: the first quantitative imaging biomarker for scleroderma. Ann Rheum Dis. 2013; 72:1845–51. [PubMed: 23426041]

Abignano G, Buch M, Emery P, Del Galdo F. Biomarkers in the management of scleroderma: an update. Curr Rheumatol Rep. 2011; 13:4–12. [PubMed: 21046295]

Boyer G, Laquieze L, Le Bot A, Laquieze S, Zahouani H. Dynamic indentation on human skin in vivo: ageing effects. Skin Res Technol. 2009; 15:55–67. [PubMed: 19152580]

Cannaò PM, Vinci V, Caviggioli F, Klinger M, Orlandi D, Sardanelli F, Serafini G, Sconfienza LM. Technical feasibility of real-time elastography to assess the peri-oral region in patients affected by systemic sclerosis. Journal of ultrasound. 2014; 17:265–69. [PubMed: 25368683]

Catheline S, Gennisson JL, Delon G, Fink M, Sinkus R, Abouelkaram S, Culioli J. Measuring of viscoelastic properties of homogeneous soft solid using transient elastography: an inverse problem approach. J Acoust Soc Am. 2004; 116:3734–41. [PubMed: 15658723]

Chen S, Urban MW, Pislaru C, Kinnick R, Zheng Y, Yao A, Greenleaf JF. Shearwave dispersion ultrasound vibrometry (SDUV) for measuring tissue elasticity and viscosity. IEEE Trans Ultrason Ferroelectr Freq Control. 2009; 56:55–62. [PubMed: 19213632]

Cicchetti DV. Guidelines, Criteria, and Rules of Thumb for Evaluating Normed and Standardized Assessment Instruments in Psychology. Psychological Assessment. 1994; 6:284–90.

Clements P, Lachenbruch P, Siebold J, White B, Weiner S, Martin R, Weinstein A, Weisman M, Mayes M, Collier D, et al. Inter and intraobserver variability of total skin thickness score (modified Rodnan TSS) in systemic sclerosis. J Rheumatol. 1995; 22:1281–5. [PubMed: 7562759]

Clements PJ, Hurwitz EL, Wong WK, Seibold JR, Mayes M, White B, Wigley F, Weisman M, Barr W, Moreland L, Medsger TA Jr, Steen VD, Martin RW, Collier D, Weinstein A, Lally E, Varga J, Weiner SR, Andrews B, Abeles M, Furst DE. Skin thickness score as a predictor and correlate of outcome in systemic sclerosis: high-dose versus low-dose penicillamine trial. Arthritis Rheum. 2000; 43:2445–54. [PubMed: 11083267]

Clements PJ, Lachenbruch PA, Ng SC, Simmons M, Sterz M, Furst DE. Skin score. A semiquantitative measure of cutaneous involvement that improves prediction of prognosis in systemic sclerosis. Arthritis Rheum. 1990; 33:1256–63. [PubMed: 2390128]

Coultas DB, Zumwalt RE, Black WC, Sobonya RE. The epidemiology of interstitial lung diseases. Am J Respir Crit Care Med. 1994; 150:967–72. [PubMed: 7921471]

Delle Sedie A, Carli L, Cioffi E, Bombardieri S, Riente L. The promising role of lung ultrasound in systemic sclerosis. Clinical rheumatology. 2012; 31:1537–41. [PubMed: 22843171]

Desai SR, Veeraraghavan S, Hansell DM, Nikolakopolou A, Goh NS, Nicholson AG, Colby TV, Denton CP, Black CM, du Bois RM, Wells AU. CT features of lung disease in patients with systemic sclerosis: comparison with idiopathic pulmonary fibrosis and nonspecific interstitial pneumonia. Radiology. 2004; 232:560–7. [PubMed: 15286324]

Garnett ES, Webber CE, Coates G, Cockshott WP, Nahmias C, Lassen N. Lung density: clinical method for quantitation of pulmonary congestion and edema. Can Med Assoc J. 1977; 116:153–4. [PubMed: 608146]

Hasegawa H, Kanai H. Improving accuracy in estimation of artery-wall displacement by referring to center frequency of RF echo. IEEE Trans Ultrason Ferroelectr Freq Control. 2006; 53:52–63. [PubMed: 16471432]

Hausermann P, Walter RB, Halter J, Biedermann BC, Tichelli A, Itin P, Gratwohl A. Cutaneous graft-versus-host disease: a guide for the dermatologist. Dermatology. 2008; 216:287–304. [PubMed: 18230976]

Hendriks FM, Brokken D, Oomens CW, Bader DL, Baaijens FP. The relative contributions of different skin layers to the mechanical behavior of human skin in vivo using suction experiments. Med Eng Phys. 2006; 28:259–66. [PubMed: 16099191]

Hou Y, Zhu QL, Liu H, Jiang YX, Wang L, Xu D, Li MT, Zeng XF, Zhang FC. A preliminary study of acoustic radiation force impulse quantification for the assessment of skin in diffuse cutaneous systemic sclerosis. J Rheumatol. 2015; 42:449–55. [PubMed: 25593239]

Iagnocco A, Kaloudi O, Perella C, Bandinelli F, Riccieri V, Vasile M, Porta F, Valesini G, Matucci-Cerinic M. Ultrasound elastography assessment of skin involvement in systemic sclerosis: lights and shadows. The Journal of rheumatology. 2010; 37:1688–91. [PubMed: 20551100]

Jahed M, Lai-Fook SJ, Bhagat PK, Kraman SS. Propagation of stress waves in inflated sheep lungs. J Appl Physiol. 1989; 66:2675–80. [PubMed: 2745329]

Kalra, S., Osborn, T., Bartholmai, B., Zhou, B., Zhang, X. Respirology. Wiley; 111 River St, Hoboken 07030-5774, NJ USA: 2017. Lung ultrasound surface wave elastography-preliminary measurements in patients with interstitial lung diseases; p. 90-90.

Khanna D, Brown KK, Clements PJ, Elashoff R, Furst DE, Goldin J, Seibold JR, Silver RM, Tashkin DP, Wells AU. Systemic sclerosis-associated interstitial lung disease-proposed recommendations for future randomized clinical trials. Clin Exp Rheumatol. 2010; 28:S55–62. [PubMed: 20576216]

Kissin EY, Schiller AM, Gelbard RB, Anderson JJ, Falanga V, Simms RW, Korn JH, Merkel PA. Durometry for the assessment of skin disease in systemic sclerosis. Arthritis Rheum. 2006; 55:603–9. [PubMed: 16874783]

Kubo K, Zhou B, Cheng Y-S, Yang T-H, Qiang B, An K-N, Moran SL, Amadio PC, Zhang X, Zhao C. Ultrasound elastography for carpal tunnel pressure measurement: A cadaveric validation study. Journal of Orthopaedic Research. 2017 n/a-n/a.

Lee SY, Cardones AR, Doherty J, Nightingale K, Palmeri M. Preliminary Results on the Feasibility of Using ARFI/SWEI to Assess Cutaneous Sclerotic Diseases. Ultrasound Med Biol. 2015; 41:2806–19. [PubMed: 26259888]

Li C, Guan G, Zhang F, Nabi G, Wang RK, Huang Z. Laser induced surface acoustic wave combined with phase sensitive optical coherence tomography for superficial tissue characterization: a solution for practical application. Biomed Opt Express. 2014; 5:1403–19. [PubMed: 24877004]

Li SC, Liebling MS, Haines KA. Ultrasonography is a sensitive tool for monitoring localized scleroderma. Rheumatology (Oxford). 2007; 46:1316–9. [PubMed: 17526926]

Liang X, Boppart SA. Biomechanical properties of in vivo human skin from dynamic optical coherence elastography. IEEE Trans Biomed Eng. 2010; 57:953–9. [PubMed: 19822464]

Lott JP, Girardi M. Practice gaps. The hard task of measuring cutaneous fibrosis. Arch Dermatol. 2011; 147:1115–6. [PubMed: 21931058]

Mathieson JR, Mayo JR, Staples CA, Muller NL. Chronic diffuse infiltrative lung disease: comparison of diagnostic accuracy of CT and chest radiography. Radiology. 1989; 171:111–6. [PubMed: 2928513]

Mayo JR. CT evaluation of diffuse infiltrative lung disease: dose considerations and optimal technique. J Thorac Imaging. 2009; 24:252–9. [PubMed: 19935222]

Merkel PA, Silliman NP, Denton CP, Furst DE, Khanna D, Emery P, Hsu VM, Streisand JB, Polisson RP, Akesson A, Coppock J, van den Hoogen F, Herrick A, Mayes MD, Veale D, Seibold JR, Black CM, Korn JH. Validity, reliability, and feasibility of durometer measurements of scleroderma skin disease in a multicenter treatment trial. Arthritis Rheum. 2008; 59:699–705. [PubMed: 18438905]

Miller GF, Pursey H. The field and radiation impedence of mechanical radiatiors on the free surface of a semi-infinite isotropic solids. Proceedings of the Royal Society of London. 1954:521–41. Series A, Mathematical and Physical Sciences.

Nguyen TM, Song S, Arnal B, Wong EY, Huang Z, Wang RK, O'Donnell M. Shear wave pulse compression for dynamic elastography using phase-sensitive optical coherence tomography. J Biomed Opt. 2014; 19:16013. [PubMed: 24441876]

Nkemzi D. A new formula for the velocity of Rayleigh waves. Wave Motion. 1997; 26:199–205.

Pailler-Mattei C, Bec S, Zahouani H. In vivo measurements of the elastic mechanical properties of human skin by indentation tests. Med Eng Phys. 2008; 30:599–606. [PubMed: 17869160]

Postlethwaite AE, Wong WK, Clements P, Chatterjee S, Fessler BJ, Kang AH, Korn J, Mayes M, Merkel PA, Molitor JA, Moreland L, Rothfield N, Simms RW, Smith EA, Spiera R, Steen V, Warrington K, White B, Wigley F, Furst DE. A multicenter, randomized, double-blind, placebo-controlled trial of oral type I collagen treatment in patients with diffuse cutaneous systemic sclerosis: I. oral type I collagen does not improve skin in all patients, but may improve skin in late-phase disease. Arthritis Rheum. 2008; 58:1810–22. [PubMed: 18512816]

Prim DA, Zhou B, Hartstone-Rose A, Uline MJ, Shazly T, Eberth JF. A mechanical argument for the differential performance of coronary artery grafts. Journal of the mechanical behavior of biomedical materials. 2016; 54:93–105. [PubMed: 26437296]

Royer D, Clorennec D. An improved approximation for the Rayleigh wave equation. Ultrasonics. 2007; 46:23–4. [PubMed: 17098270]

Serup, J., Jemec, GBE. Handbook of non-invasive methods and the skin. Boca Raton: CRC press; 1995.

Shazly T, Rachev A, Lessner S, Argraves WS, Ferdous J, Zhou B, Moreira AM, Sutton M. On the uniaxial ring test of tissue engineered constructs. Experimental Mechanics. 2015; 55:41–51.

Smalls LK, Randall Wickett R, Visscher MO. Effect of dermal thickness, tissue composition, and body site on skin biomechanical properties. Skin Res Technol. 2006; 12:43–9. [PubMed: 16420538]

Spentzouris G, Labropoulos N. The evaluation of lower-extremity ulcers. Semin Intervent Radiol. 2009; 26:286–95. [PubMed: 21326538]

Steen VD, Medsger TA. Changes in causes of death in systemic sclerosis, 1972–2002. Ann Rheum Dis. 2007; 66:940–4. [PubMed: 17329309]

Steen VD, Medsger TA Jr. Severe organ involvement in systemic sclerosis with diffuse scleroderma. Arthritis Rheum. 2000; 43:2437–44. [PubMed: 11083266]

Steen VD, Medsger TA Jr. Improvement in skin thickening in systemic sclerosis associated with improved survival. Arthritis Rheum. 2001; 44:2828–35. [PubMed: 11762943]

Twal WO, Klatt SC, Harikrishnan K, Gerges E, Cooley MA, Trusk TC, Zhou B, Gabr MG, Shazly T, Lessner SM. Cellularized microcarriers as adhesive building blocks for fabrication of tubular tissue constructs. Annals of biomedical engineering. 2014; 42:1470–81. [PubMed: 23943070]

Van Hattem S, Bootsma AH, Thio HB. Skin manifestations of diabetes. Cleve Clin J Med. 2008; 75:772, 74. 76–7 passim. [PubMed: 19068958]

Verschakelen JA. The role of high-resolution computed tomography in the work-up of interstitial lung disease. Curr Opin Pulm Med. 2010; 16:503–10. [PubMed: 20644479]

Viktorov, I. Raleigh and Lamb Waves. New York: Plenum Press; 1976.

Vinh PC, Malischewsky PG. An improved approximation of Bergmann's form for the Rayleigh wave velocity. Ultrasonics. 2007; 47:49–54. [PubMed: 17825868]

Wells AU, Hansell DM, Rubens MB, Cullinan P, Black CM, du Bois RM. The predictive value of appearances on thin-section computed tomography in fibrosing alveolitis. Am Rev Respir Dis. 1993; 148:1076–82. [PubMed: 8214928]

Zachary JF, Blue JP Jr, Miller RJ, Ricconi BJ, Eden JG, O'Brien WD Jr. Lesions of ultrasound-induced lung hemorrhage are not consistent with thermal injury. Ultrasound Med Biol. 2006; 32:1763–70. [PubMed: 17112962]

Zhang X, Greenleaf JF. Estimation of tissue's elasticity with surface wave speed. J Acoust Soc Am. 2007; 122:2522–5. [PubMed: 18189542]

Zhang X, Osborn T, Kalra S. A noninvasive ultrasound elastography technique for measuring surface waves on the lung. Ultrasonics. 2016; 71:183–8. [PubMed: 27392204]

Zhang X, Osborn T, Zhou B, Bartholmai B, Greenleaf JF, Kalra S. An ultrasound surface wave elastography technique for noninvasive measurement of surface lung tissue. The Journal of the Acoustical Society of America. 2017; 141:3721–21.

Zhang X, Osborn TG, Pittelkow MR, Qiang, Kinnick RR, Greenleaf JF. Quantitative assessment of scleroderma by surface wave technique. Medical Engineering & Physics. 2011; 33:31–37. [PubMed: 20888282]

Zhang X, Qiang B, Hubmayr RD, Urban MW, Kinnick R, Greenleaf JF. Noninvasive ultrasound image guided surface wave method for measuring the wave speed and estimating the elasticity of lungs: A feasibility study. Ultrasonics. 2011; 51:289–95. [PubMed: 20971489]

Zhou B, Sit AJ, Zhang X. Noninvasive measurement of wave speed of porcine cornea in ex vivo porcine eyes for various intraocular pressures. Ultrasonics. 2017; 81:86–92. [PubMed: 28618301]

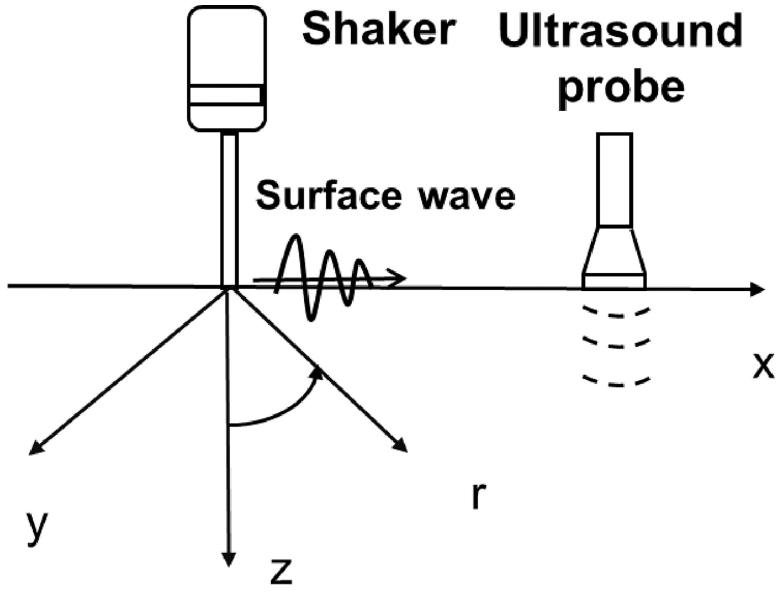

Figure 1.

Schema of surface wave generation and detection on the skin. The skin surface is on the plane of x and y coordinates. The surface wave on the skin is generated by a handheld electromechanical shaker through a ball-tip applicator on the skin. The vibration excitation is typically 0.1 second harmonic signal at a frequency between 100 Hz and 200 Hz. The resulting surface wave propagation on the skin is measured using an ultrasound probe. A standoff gel pad is used between the ultrasound probe and skin to improve imaging of the skin. The surface wave speed depends on the local elastic properties of the skin and independent of the location of wave generation.

Figure 2.

Schematic of skin locations tested on human subjects. Square box indicates the tested positions. Probe orientation is aligned with the arm longitudinal axis. Left and right forearms and upper arms were labelled as L4, L5, R4, and R5.

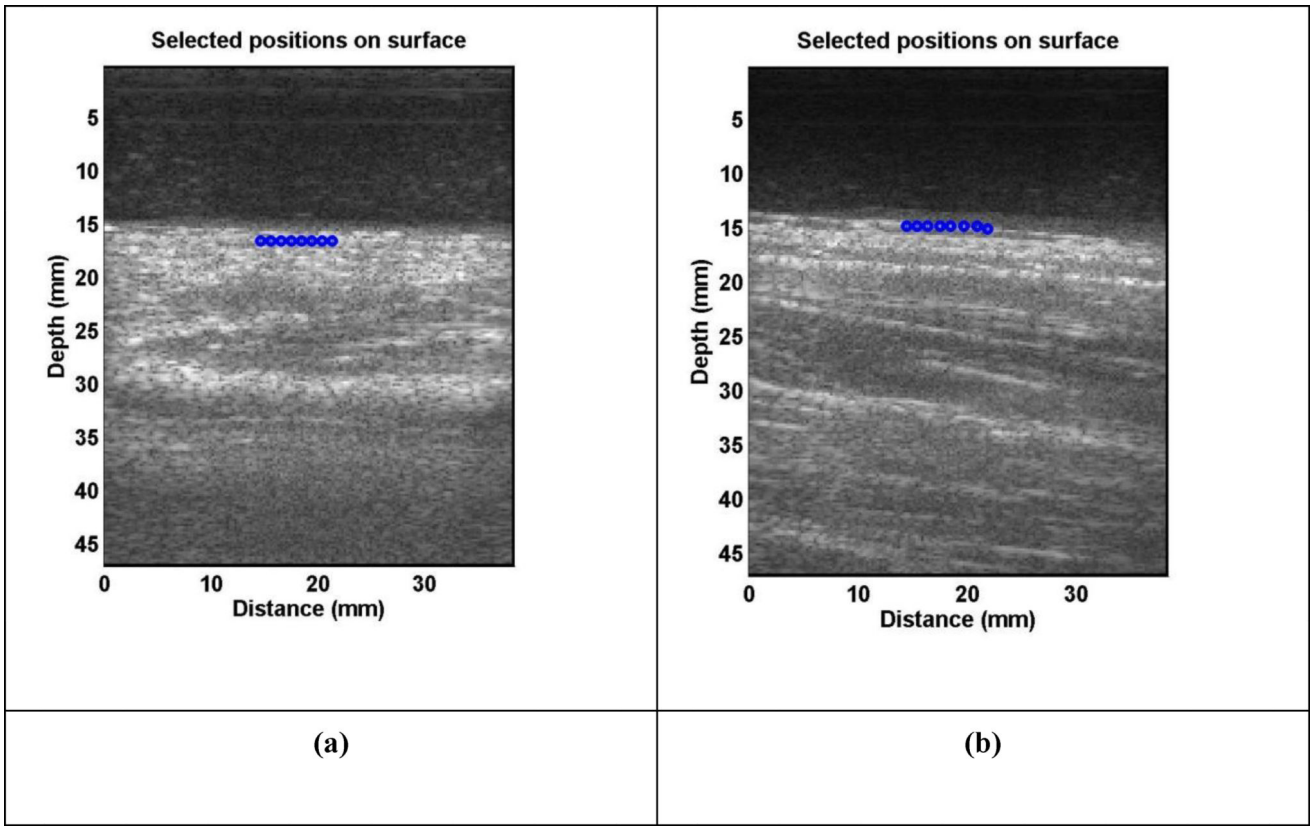

Figure 3.

Representative B-mode images of skin for a patient (a) and a healthy subject (b). An ultrasound gel pad standoff was used to improve imaging of the skin. The top dark area in the image was associated with the gel pad. Eight locations on the skin surface were used to measure the surface wave speed of skin.

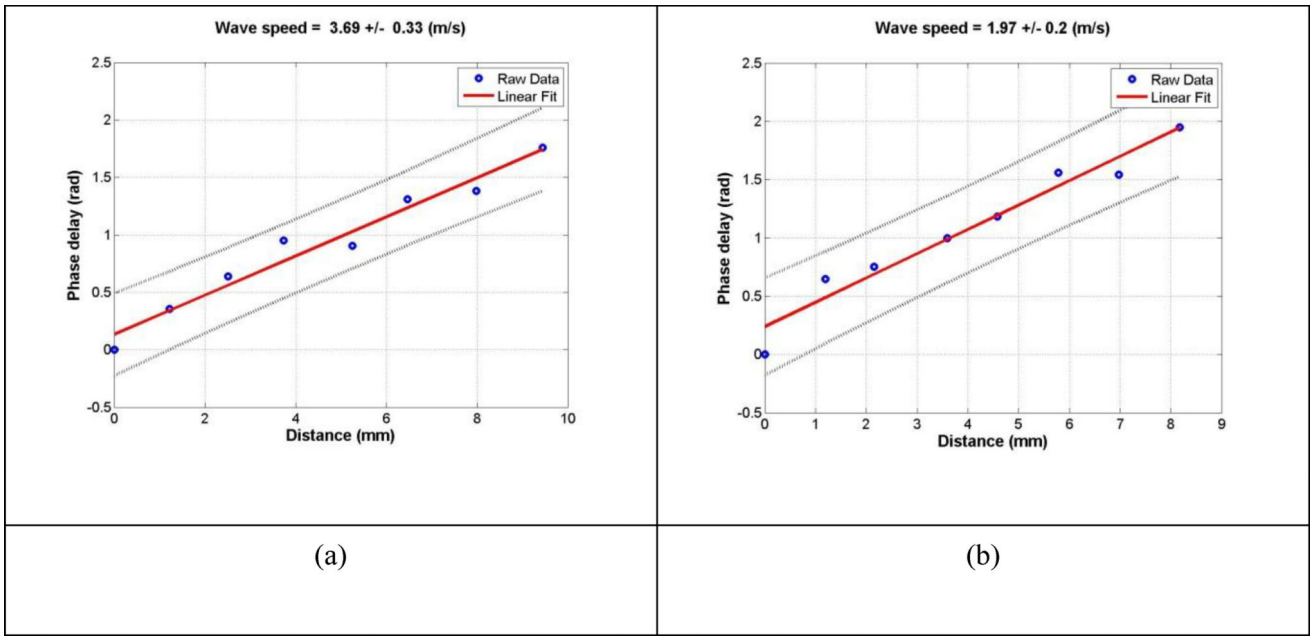

Figure 4.

The wave phase delay of the remaining locations, relative to the first location, is used to measure the surface wave speed. The slope of phase delay with distance measures the wave speed using equation (7). Representative examples of wave speed at 100 Hz for a patient (a) and a healthy subject (b).

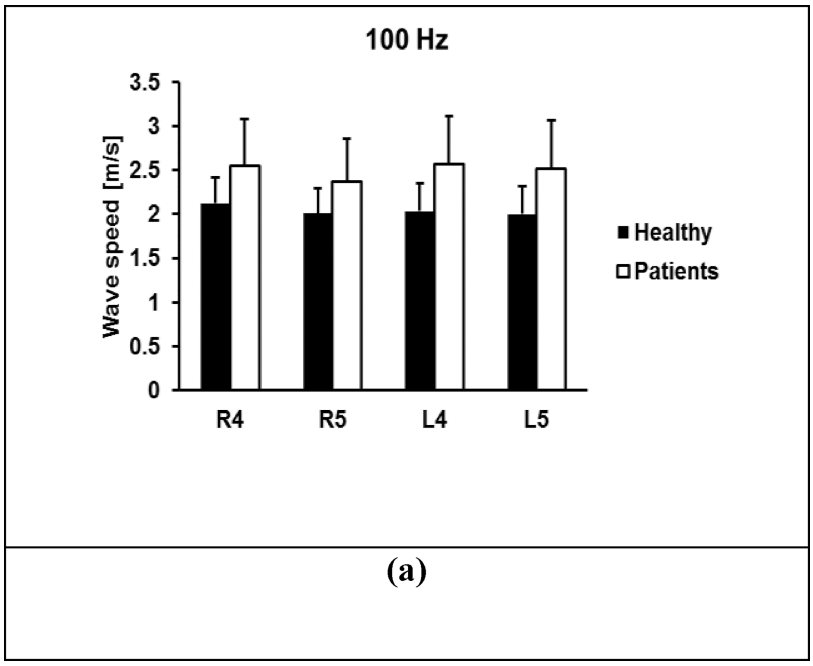

(a)

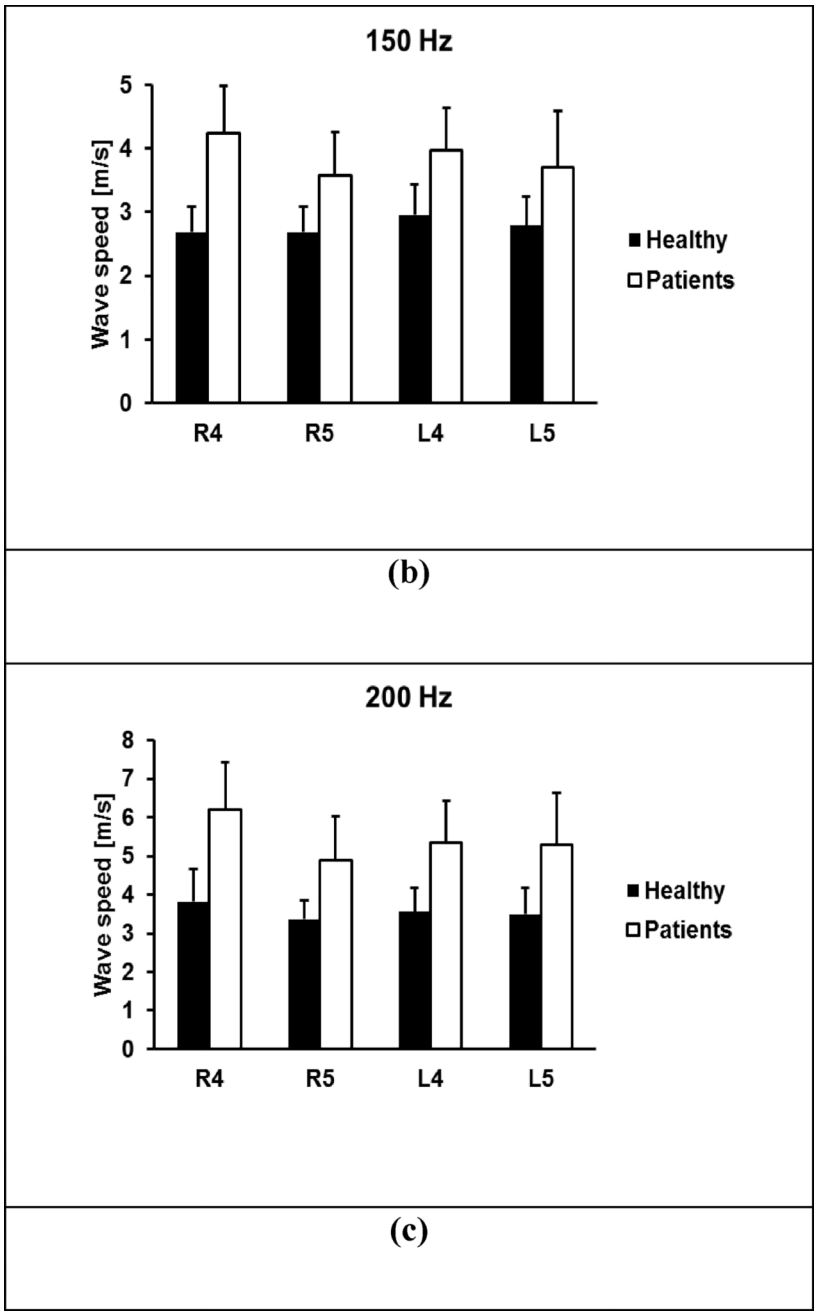

Figure 5.

Comparison of wave speeds between healthy subjects and patients at four locations. Surface wave speeds at (a) 100 Hz, (b) 150 Hz, (c) 200 Hz. The p-values were less than 0.0001 for all four locations and three frequencies between the patients and controls, respectively.

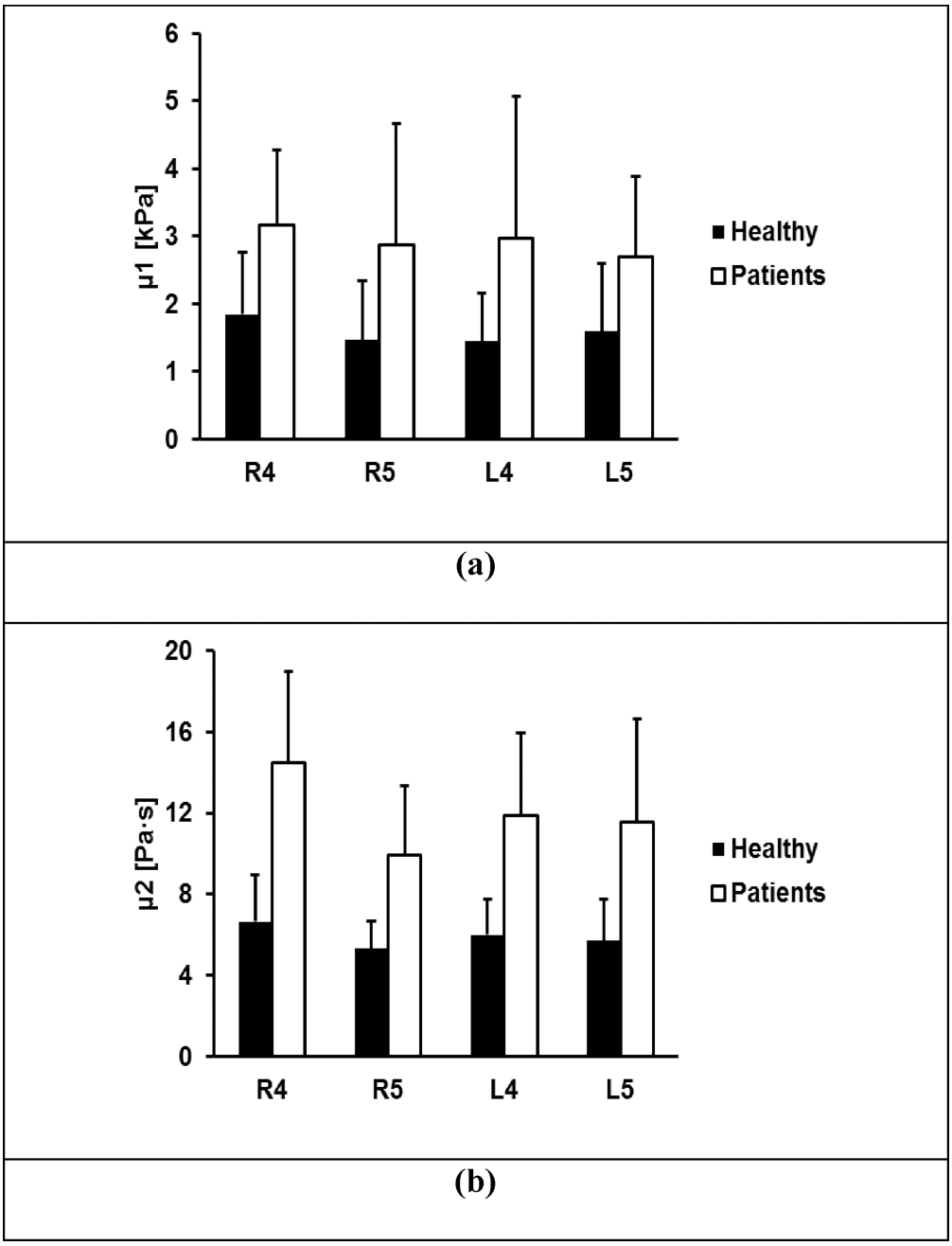

Figure 6.

Comparison of elasticity μ1 (a) and viscosity μ2 (b) between healthy subjects and patients at four locations. The p-values were less than 0.0001 for the four locations between the patients and controls.

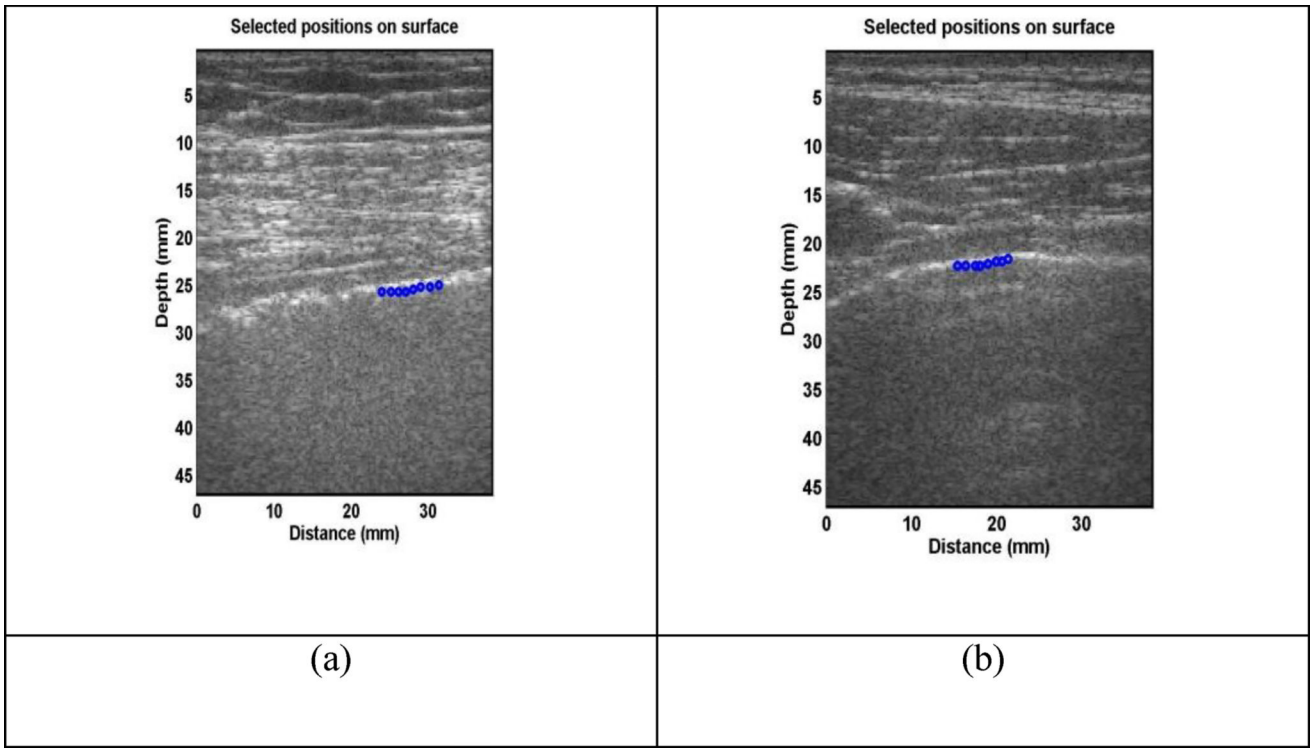

Figure 7.
Representative B-mode images of a lung for a patient (a) and a healthy subject (b). The lung surface of a healthy subject is typically smooth while a patient's lung surface is relatively rough.

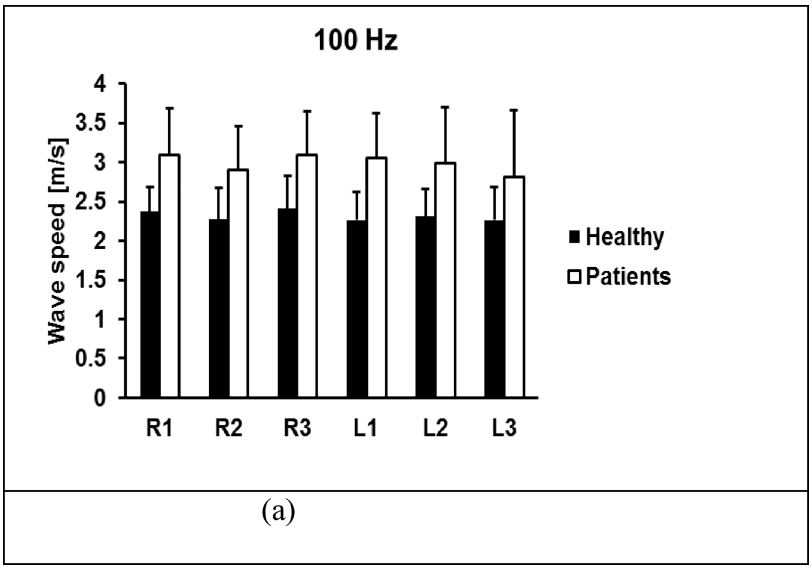

(a)

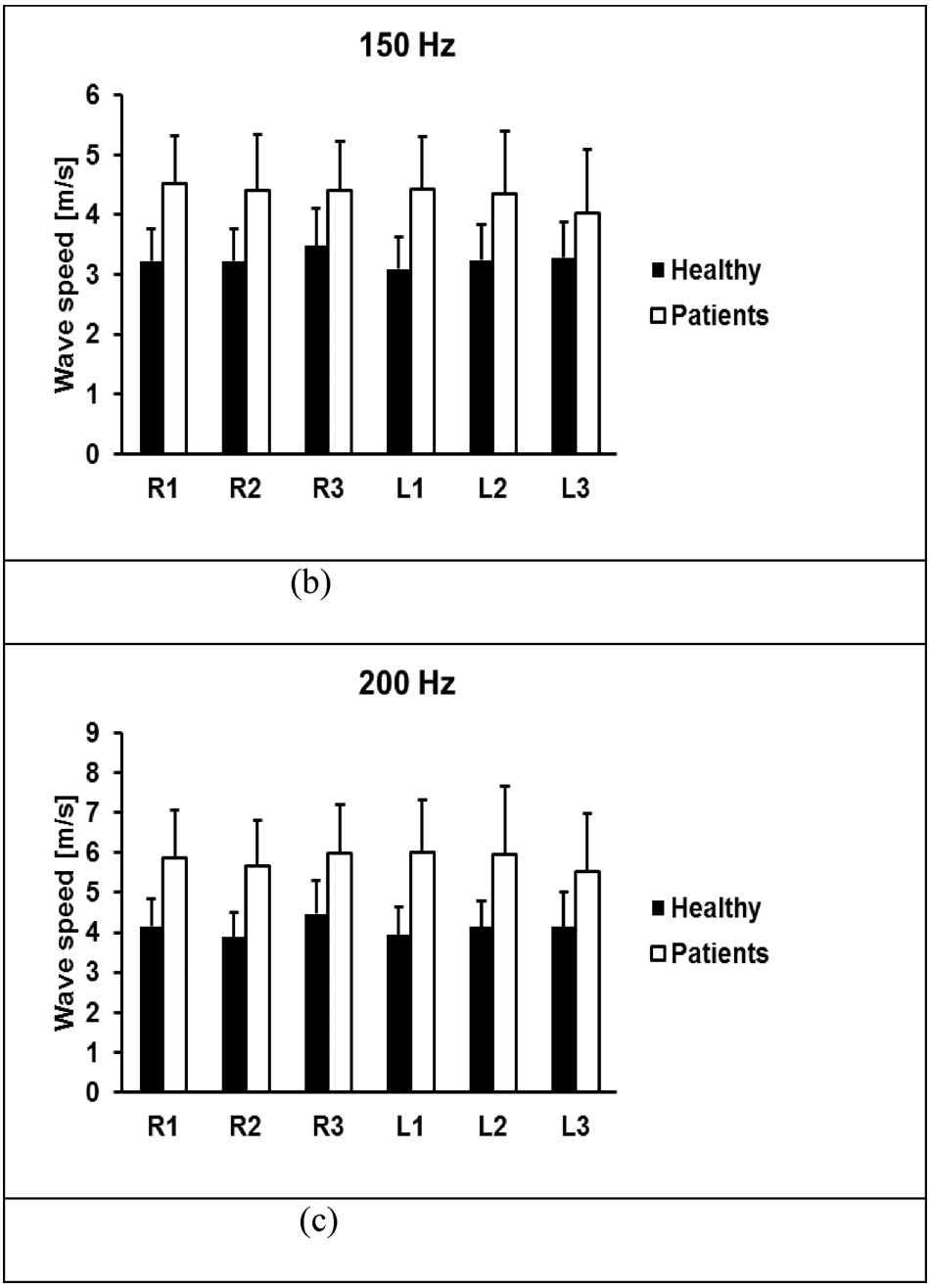

Figure 8.

Comparison of wave speeds between healthy subjects and patients through six intercostal spaces. Surface wave speeds were measured at (a) 100 Hz, (b) 150 Hz, (c) 200 Hz. The p-values were less than 0.0001 for all intercostal spaces and for three frequencies between the patients and controls.

Table 1

Representative surface wave speeds of a healthy subject and a patient at four locations of skin at 100 Hz, 150 Hz and 200 Hz.

Healthy [m/s]	**R4**	**R5**	**L4**	**L5**
100 Hz	1.97 ± 0.31	1.7 ± 0.28	1.83 ± 0.04	1.79 ± 0.07
150 Hz	2.31 ± 0.08	2.5 ± 0.13	2.33 ± 0.25	2.52 ± 0.41
200 Hz	2.82 ± 0.19	2.99 ± 0.18	3.04 ± 0.37	3 ± 0.19
Patients	**R4**	**R5**	**L4**	**L5**
100 Hz	3.42 ± 0.27	2.22 ± 0.25	2.82 ± 0.31	2.47 ± 0.22
150 Hz	4.52 ± 0.59	2.52 ± 0.35	3.6 ± 0.38	3.67 ± 0.25
200 Hz	5.17 ± 0.57	3.04 ± 0.23	5.36 ± 0.55	5.78 ± 0.64

Table 2

Representative surface wave speeds of a healthy subject and a patient through six intercostal spaces at 100 Hz, 150 Hz and 200 Hz.

healthy [m/s]	**R1**	**R2**	**R3**	**L1**	**L2**	**L3**
100	1.98 ± 0.07	1.83 ± 0.26	2.01 ± 0.23	2.07 ± 0.39	2.09 ± 0.3	1.95 ± 0.32
150	2.63 ± 0.46	2.65 ± 0.15	2.56 ± 0.16	2.61 ± 0.16	2.68 ± 0.12	2.52 ± 0.42
200	3.18 ± 0.58	3.28 ± 0.25	3.14 ± 0.13	2.98 ± 0.36	3.03 ± 0.2	3.1 ± 0.45
patient [m/s]	**R1**	**R2**	**R3**	**L1**	**L2**	**L3**
100	3.26 ± 0.41	2.78 ± 0.34	3.25 ± 0.15	2.8 ± 0.39	2.79 ± 0.95	2.97 ± 0.26
150	3.86 ± 0.43	3.59 ± 0.41	4.36 ± 0.43	3.35 ± 0.61	3.13 ± 0.85	3.57 ± 0.02
200	4.19 ± 1.61	4.57 ± 0.13	5.79 ± 0.64	5.51 ± 0.51	4.63 ± 1.27	4.35 ± 1.03